

Field-induced linear magnetoelastic coupling in multiferroic TbMnO₃

N. Aliouane,¹ D. N. Argyriou,¹ J. Stropfer,² I. Zegkinoglou,² S. Landsgesell,¹ and M. v. Zimmermann³
¹Hahn-Meitner-Institut, Glienicker Strasse 100, Berlin D-14109, Germany

²Max-Planck-Institut für Festkörperforschung, Heisenbergstraße 1, 70569 Stuttgart, Germany

³Hamburger Synchrotronstrahlungslabor HASYLAB at Deutsches Elektronen-Synchrotron DESY,
 Notkestraße 85, 22603 Hamburg, Germany

(Received 20 August 2005; published 3 January 2006)

We have used in-field neutron and x-ray single-crystal diffraction to measure the incommensurability δ of the crystal and magnetic structures of multiferroic TbMnO₃. We show that the flop in the electric polarization at the critical field H_C , for field H along the a and b axes, coincides with a first-order transition to a commensurate phase with propagation vector $\kappa=(0, \frac{1}{4}, 0)$. In-field x-ray diffraction measurements show that the quadratic magnetoelastic coupling breaks down with applied field as shown by the observation of the first harmonic lattice reflections above and below H_C . This indicates that magnetic field induces a linear magnetoelastic coupling.

DOI: 10.1103/PhysRevB.73.020102

PACS number(s): 77.80.Bh, 64.70.Kb, 75.25.+z, 77.22.Ej

Control of the spontaneous ferroelectric polarization (P_s) with an external magnetic field (H) in a material opens the opportunity for new types of magnetoelectric devices. The realization of such devices is based on multiferroic materials in which magnetism and ferroelectricity are strongly coupled. While available multiferroics are limited, it has been shown that frustrated spin materials may offer a unique class of enhanced multiferroics.¹⁻³ In one of these materials, TbMnO₃, we find that multiferroic behavior arises as a consequence of the release of frustration with H . Here ferroelectricity arises below the Néel temperature (T_N) from a coupling to the lattice of an incommensurate (IC) modulation of the magnetic structure [Fig. 1(a)] that is caused from frustration in the ordering of the Mn d orbitals.^{1,3} In this communication we show that magnetic field releases this frustration, inducing a linear magnetoelastic coupling, so that ferroelectricity is no longer a secondary effect. The linear magnetoelastic coupling drives a magnetostructural transition from an IC phase, which has P_s along the c axis ($P\parallel c$), to a commensurate (C) phase with P_s along the a axis ($P\parallel a$).

In TbMnO₃, when a magnetic field is applied along the b axis ($H\parallel b$) at 2 K, parallel to the direction of the IC magnetic modulation [see Fig. 1(a)], the electric polarization of the lattice flops from $P\parallel c$ to $P\parallel a$ at the critical field $H_C^b \sim 4.5$ T [Fig. 2(d)]. When field is applied along the a axis ($H\parallel a$), perpendicular to the magnetic modulation, a similar flop is found but at a higher critical field, $H_C^a \sim 9$ T [Fig. 2(a)]. Recently there have been a number of examples of magnetoelastic coupling in complex multiferroic oxides such as TbMn₂O₅ which exhibit a reversible polarization switch with applied field,⁴ and hexagonal HoMnO₃ where one magnetic phase is selected over another by applying an electric field.⁵ However, TbMnO₃ is unique as it is the only known example of a material that exhibits a field-induced flop of its polarization.

In TbMnO₃ the staggered ordering of Mn³⁺ $3d_{3x^2-r^2}/3d_{3y^2-r^2}$ orbitals as found in LaMnO₃ is frustrated partly due to the small ionic size of Tb³⁺. This leads to an IC spin ordering which drives a ferroelectric lattice modulation.^{3,6} The wave vector for the modulation of the Mn

spins is $\kappa_m^{\text{Mn}}=(0, k \pm \delta_m^{\text{Mn}}, 0)$, with incommensurability $\delta_m^{\text{Mn}} \sim 0.29$ at T_N (first harmonic).^{7,8} Accompanying the magnetic ordering there is a lattice modulation with $\delta_l=2\delta_m$ (second harmonic)¹⁻³ consistent with a *quadratic magnetoelastic coupling* between the lattice and the spin-density wave.^{9,10} Below $T_N^{\text{Tb}}=7$ K, sinusoidal Tb spin order is also found [$\kappa_m^{\text{Tb}}=(0, k \pm \delta_m^{\text{Tb}}, 0)$, $\delta_m^{\text{Tb}}=0.42$] (Ref. 8) and is expected to produce a similar coupling to the lattice with $\delta_m^{\text{Tb}}=2\delta_l^{\text{Tb}}$.

To uncover the nature of the coupling between P and H we have used in-field neutron and synchrotron x-ray single-crystal diffraction to measure the field response of δ with $H\parallel a$ and $H\parallel b$, up to 14 T. Single crystals were obtained by recrystallizing a ceramic rod of TbMnO₃ under Ar atmo-

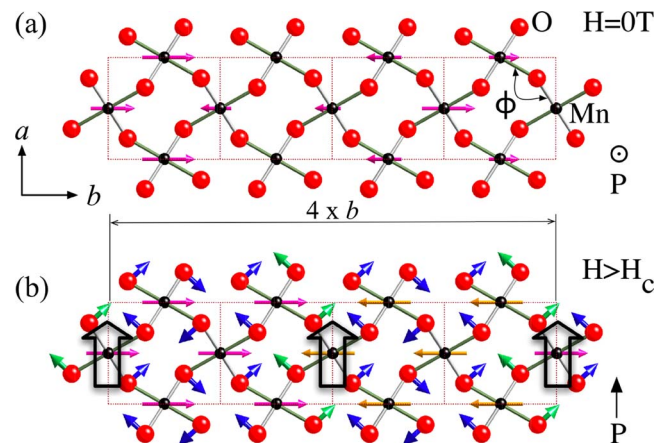


FIG. 1. (Color online) Crystal and magnetic structures of TbMnO₃ ($Pbnm$, $a=5.302$, $b=5.857$, $c=7.402$ Å) in the ab plane. Long (darker) and short (lighter) Mn-O bond ordering arises from staggered $3d_{3x^2-r^2}/3d_{3y^2-r^2}$ orbital ordering found above T_N . (a) A model of the IC magnetic structure of TbMnO₃ below T_N (Ref. 7). The arrows through Mn atoms indicate the direction of Mn spins. (b) A model of the Mn spin structure for TbMnO₃ for $H > H_C$. Here arrows from O atoms indicate the direction of displacement from the average structure as to increase (decrease) the angle ϕ on the basis of FM (AFM) coupling between adjacent Mn ions. The large arrows on ferroelectrically active octahedra indicate the direction of the predicted polarization from these displacements.

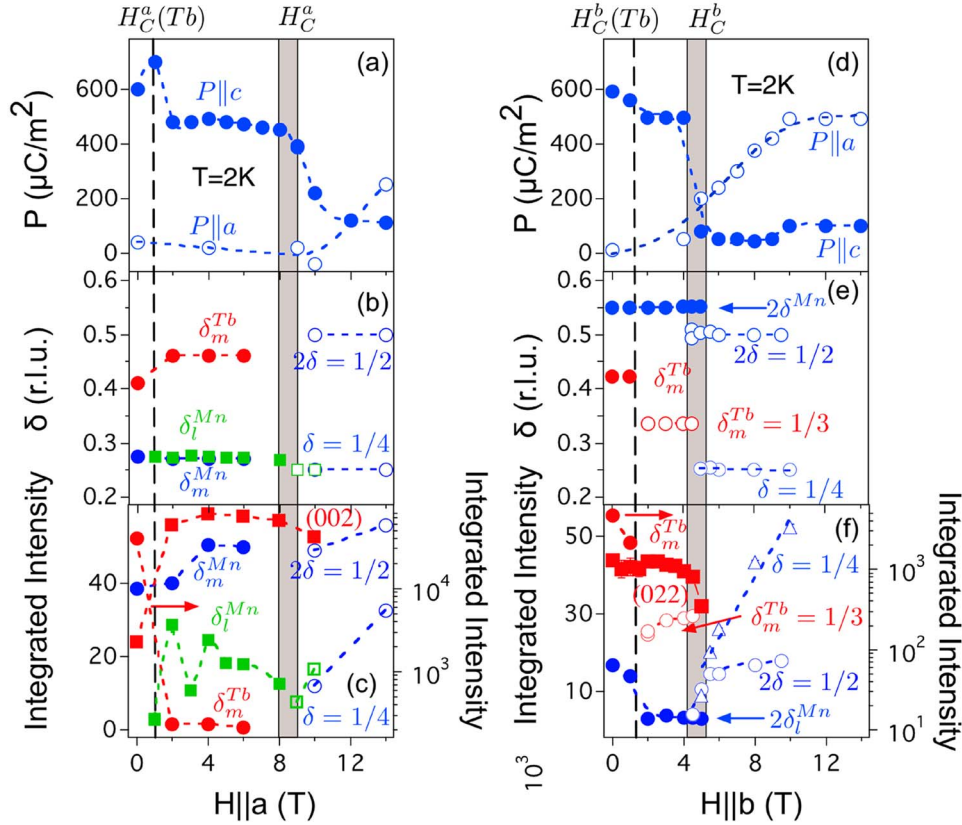


FIG. 2. (Color online) (a,d) Electric polarization $P||a$ and $P||c$ of TbMnO_3 for $H||a$ and $H||b$. These data were compiled from field-cooled measurements reported by Kimura *et al.* (Ref. 11). (b) Variation of δ as a function of $H||a$ for reflections $(0, \delta_m^{\text{Mn}}, 1)$, $(0, \delta_m^{\text{Tb}}, 1)$ measured using neutron diffraction (filled blue and red circles, respectively) and $(0, 3-\delta, 8)$ measured with x-ray diffraction (filled green squares). For $H > H_C^a$ the C reflections $(0, \frac{1}{2}, 1)$ and $(0, \frac{1}{2}, 1)$ (open blue circles) were measured using neutron diffraction while the $(0, 2\frac{3}{4}, 8)$ reflection with x rays (open green squares). (c) Variation of the integrated intensity as a function of $H||a$ for the same reflections as in panel (b). For the $(0, \delta_m^{\text{Tb}}, 1)$ reflection the logarithmic scale on the right axis is used. The field dependence of the intensity of the FM (002) reflection is also shown (filled red squares). (e) Variation of δ as a function $H||b$, for the $(0, \delta_m^{\text{Tb}}, 1)$ reflection and the C reflection $(0, \frac{1}{3}, 1)$ due to Tb spin ordering (filled and unfilled red circles, respectively). On the same panel we show the results of x-ray diffraction measurements of the $(0, 2\delta^{\text{Mn}}, 3)$ reflection (filled blue circles) and the C reflections $(0, \frac{1}{2}, 3)$ and $(0, \frac{1}{4}, 3)$ (open blue circles). (f). Variation of the integrated intensity as a function of $H||b$ for the reflections shown in panel (e). For the $(0, \delta_m^{\text{Tb}}, 1)$ reflection the logarithmic scale on the right axis is used. The field dependence of the intensity of the FM (022) reflection is also shown (filled red squares). Integrated intensity in panels (c) and (d) are shown in arbitrary units. All measurements are taken at 2 K.

sphere using an optical floating zone furnace. Small pieces of our crystal were characterized using magnetization and specific heat in good agreement with published measurements.^{1,11} Synchrotron x-ray diffraction measurements were carried out on beamline X21 ($E_i=9.5$ keV) at the NSLS, Brookhaven National Laboratory, using a vertical 13-T superconducting magnet with the sample aligned with $H||a$, and at the BW5 beamline at HASYLAB ($E_i=100.5$ keV), using a horizontal 10-T superconducting magnet and the sample aligned with $H||b$. Neutron-diffraction experiments were made on a single crystal of TbMnO_3 at the BENS facility of the Hahn-Meitner Institut, Berlin. For measurements with $H||a$ we used the FLEX cold triple-axis spectrometer with a collimation of $40'-40'-40'$, $k_i=1.5 \text{ \AA}^{-1}$, and a cooled Be filter on the scattered beam, while a magnetic field was applied using the vertical 14.5-T superconducting magnet VM1. For measurements with $H||b$ we used the two-axis diffractometer E4 ($\lambda=2.2 \text{ \AA}$) with a $60'-40'$ collimation while field was applied using the 4-T horizontal field magnet HM1. In all cases diffraction measurements

were made in the bc plane. Our neutron-diffraction measurements are sensitive to magnetic ordering whereas x-ray diffraction experiments probe the lattice.

With $H||a$ we measured characteristic reflections using neutron diffraction by cooling our crystal from 50 to 2 K in fields of 0, 2, 4, 6, 10, and 14 T. The variation of δ for Mn and Tb spin ordering as a function of field at 2 K, compiled from these measurements, is shown in Fig. 2(b), while the variation of the intensity of the same reflections is shown in Fig. 2(c).

In Fig. 3(b) we show neutron-diffraction scans through the first harmonic reflection $(0, \delta_m^{\text{Mn}}, 1)$ as a function of $H||a$. The intensity of this reflection is enhanced with H from 2 to 4 T while the magnitude of δ_m^{Mn} remains unchanged for fields up to 8 T [Figs. 2(b) and 2(c)]. However, for $H > H_C^a \sim 9$ T we find that δ of the first harmonic reflection has changed to a C value of $\delta=\frac{1}{4}$ and is accompanied by a second harmonic reflection with $2\delta=\frac{1}{2}$ [Fig. 2(b)]. This transition at H_C^a coincides with the polarization flop from $P||c$ to $P||a$ as shown in Fig. 2(a). The implication of this observation is that the po-

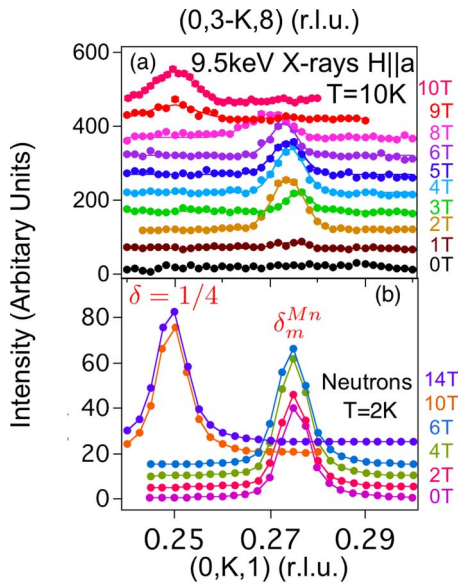


FIG. 3. (Color online) (a) X-ray diffraction scans of the first harmonic $(0,3-K,8)$ reflection as a function of field with $H\parallel a$ at $T=10$ K, measured on X21. (b) Neutron-diffraction scans through the first harmonic $(0, \delta_m^{\text{Mn}}, 1)$ reflection as a function of $H\parallel a$.

larization flop arises because the spontaneous polarization of the C phase is along the a axis, different from that of the IC phase.

In Fig. 3(a) we show x-ray diffraction scans as a function of $H\parallel a$ at $T=10$ K for the first harmonic $(0,3-\delta^{\text{Mn}},8)$ reflection. If the magnetoelastic coupling is quadratic, then only magnetic scattering is allowed for this reflection, and indeed we do not observe a signal at this position for $H\parallel a < 2$ T. However, for $H\parallel a \geq 2$ T a peak becomes visible and above H_C^a it locks into the C value of $\delta = \frac{1}{4}$. The observation of a lattice reflection at the wave vector of the first harmonic indicates that for $H\parallel a$ a linear magnetoelastic coupling is induced above 2 T which is maintained above H_C into the C phase. The variation of the intensity of this reflection shown in Fig. 2(c) is complex, but its changes are associated with the metamagnetic transition of Tb spins (see below) and the increase in the intensity of the first harmonic reflection $(0, \delta_m, 1)$ between 2 and 4 T [see Fig. 2(c)].

The behavior of the Tb magnetic reflections is significantly different from that of Mn for $H\parallel a$. For example, the intensity of the $(0, \delta_m^{\text{Tb}}, 1)$ reflection decreases by two orders of magnitude between 0 and 2 T [Fig. 2(c)], indicative of a metamagnetic transition¹ and coincides with a rapid increase in the intensity of the ferromagnetic (FM) (002), (020), and (011) reflections at low temperature [see Fig. 2(c)]. This indicates that for $H\parallel a$ the application of field results in the FM alignment of Tb spins, leading to a significant decrease in the magnitude of the IC-spin component. The FM ordering of Tb spins would greatly diminish their influence over the ferroelectric properties of TbMnO₃ for this field configuration. Above H_C^a we find no evidence of IC Tb spin ordering.

The polarization flop, when the field is applied along the b axis in the direction of the magnetic modulation, occurs at a lower critical field of $H_C^b \sim 4$ T [Fig. 2(d)]. Here we applied a magnetic field parallel to the b axis after the sample was

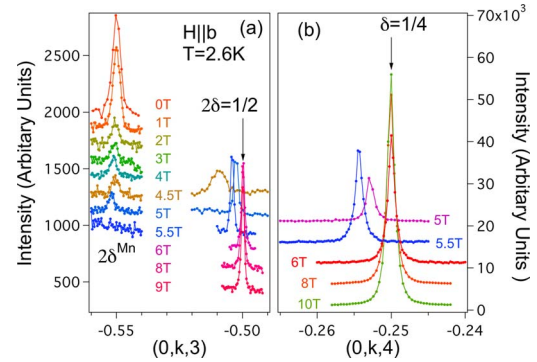


FIG. 4. (Color online) (a) Scans of the second harmonic IC lattice reflection at $(0, 2\delta^{\text{Mn}}, 3)$ with increasing field at 2.6 K measured on BW5. The C reflection at $(0, \frac{1}{2}, 3)$ is shown for $H > H_C^b$. (b) Similarly, scans of the first harmonic $(0, \frac{1}{4}, 4)$ reflection of the C phase with increasing field at 2.6 K for $H > H_C^b$ are shown.

cooled to 2 K in zero field, and characteristic superlattice reflections, such as the $(0, 2\delta^{\text{Mn}}, 3)$, were measured using x-ray diffraction (see Fig. 4). When a magnetic field is applied, the incommensurability of the second harmonic reflection remains invariant [Fig. 2(e)] but its intensity rapidly decreases with field from 0 to 2 T and remains low up to ~ 4 T [Fig. 2(f)]. Increasing field clearly destabilizes the lattice modulation and leads to a discontinuous transition to the C phase with $2\delta = \frac{1}{2}$ at $H_C^b = 4.5$ T [Figs. 2(e), 2(f), and 4(a)]. We find C and IC reflections coexisting over the field range of 4–5.5 T, while for $H > 5.5$ T only the $2\delta = \frac{1}{2}$ superlattice reflection is visible [Fig. 4(a)]. Coincident to this magnetostructural transition is the polarization flop from $P\parallel c$ to $P\parallel a$ at about 4.5 T as shown in Fig. 2(d).

As with the previous field configuration, here our x-ray measurements also revealed superlattice reflections with $\delta = \frac{1}{4}$ above H_C^b [Figs. 2(e), 2(f), and 4(b)]. The linear increase in the intensity of this reflection with $H\parallel b$ above H_C^b is particularly striking, as it mirrors a linear increase in $P\parallel a$ [Fig. 2(d)] between 4 and 10 T. This linear increase in $P\parallel a$ is indicative of a linear magnetoelectric coupling in the C phase. The variation of intensity with field of the second harmonic reflection is different in that it increases rapidly above H_C^b and shows a constant variation with H above ~ 6 T [Fig. 2(f)].

For this field configuration we find, using neutron diffraction, that at 2 K Tb spins undergo an additional discontinuous transition to a C phase with $\delta_m^{\text{Tb}} = \frac{1}{3}$ at $H\parallel b = 1.25$ T, as shown in Fig. 2(e). From symmetry analysis Tb spins for this phase are both sign and amplitude modulated. This transition is reflected in an anomaly in $P\parallel c$ at the same field value [Fig. 2(d)], and a significant increase in the magnetization at this temperature is also reported.¹ However, unlike the $H\parallel a$ case, here field neither suppresses the intensity of the IC Tb reflections nor does it enhance the FM component [Fig. 2(f)]. Above H_C^b we find no evidence of IC ordering of Tb spins while the FM intensity appears to decrease.

In zero field TbMnO₃ is an improper ferroelectric where the lattice polarization arises from a quadratic magnetoelastic coupling to a spin-density wave, as indicated by the observation of second harmonic structural reflections.^{9,10} Here we

demonstrate that this picture of improper ferroelectricity in TbMnO_3 breaks down with H even below H_C for the case of $H\parallel a$ and most likely for $H\parallel b$. The identical periodicity of the magnetic and crystal structures indicates that H switches on a linear magnetoelastic coupling which is maintained into the C phase. This would suggest that the IC–C phase transition we report on, and consequently the polarization flop at H_C , are driven by field-induced linear magnetoelastic coupling. Our measurements clarify the role of Tb spins on the polarization flop at H_C . For $H\parallel a$ Tb spins show a FM alignment well below H_C^a and only a smaller IC component, and thus are not expected to contribute to the polarization flop strongly. For $H\parallel b$, however, the situation is more complex as Tb spins exhibit an additional transition to the $\delta_m^{\text{Tb}} = \frac{1}{3}$ phase, while a strong FM enhancement is not observed. Together with the lower critical field for $H\parallel b$ the polarization flop here may be driven by an interplay between Mn and Tb spin ordering as suggested by Kimura *et al.*¹

The *magnetolectric* coupling is expected to change in a similar way as the magnetoelastic coupling. Indeed the behavior of TbMnO_3 with H is reminiscent of that of BiFeO_3 , which exhibits a switch to linear magnetoelastic coupling at ~ 20 T (Refs. 12 and 13). The coupling between P and H is expressed by $P_i = P_{si} + \alpha_{ij}H_j + \frac{1}{2}\beta_{ijk}H_jH_k$, where P_s is the spontaneous polarization, α_{ij} is the tensor of the magneto-electric susceptibility, and β_{ijk} is a tensor describing the coupling of a spiral and/or cycloid magnetic structure to the lattice.^{12,13} In an analogy to BiFeO_3 , we suggest that as field destroys the spiral spin ordering (β_{ijk} is renormalized), a linear magnetolectric effect would be expected to arise.^{12,14} Indeed a linear behavior in P versus H is evident for $H\parallel b$ [Fig. 2(d)].

The propagation vector of $\kappa = (0, \frac{1}{4}, 0)$ uniquely gives a spin structure that is only sign modulated as depicted in Fig. 1(b). It is important to consider the effect of this magnetic ordering on the frustrated orbital ordering. The crystal structure of TbMnO_3 ($H=0$ T, $T > T_N$) shows an ordering of long and short bonds as found in LaMnO_3 , but with a low angle ϕ of 144° between MnO_6 octahedra (Mn–O–Mn), compared to 165° found in LaMnO_3 (Ref. 15). A simple application of Goodenough's rules would suggest a layered antiferromagnetic (AFM) ordering, inconsistent with the present data.¹⁶ We propose here that the structural distortion that is coupled to the $\uparrow\uparrow\downarrow\downarrow$ spin structure arises from the ordering of ϕ . Small values of ϕ would result in AFM interactions between adjacent Mn spins as the influence of superexchange via t_{2g} orbitals would be more significant.^{3,16} On the other hand, a relative larger value of ϕ will be less influenced from t_{2g}

interactions and would propagate a FM coupling between Mn spins as it does in LaMnO_3 . Indeed the layered AFM structure is stable to values of ϕ as low as 148° , found in SmMnO_3 (Ref. 3). Using the magnetic ordering of the high-field C phase as a constraint and displacing O atoms in the paraelectric structure so that ϕ should increase (decrease) for FM (AFM) coupling between adjacent Mn spins, one arrives at a structural model shown in Fig. 1(b). The result is a structure where ferromagnetically coupled MnO_6 octahedra undergo simple rotations (ferroelectrically inactive), while octahedra that are frustrated by AFM coupling in the ab plane show a scissorlike distortion (ferroelectrically active). The combined rotations and scissorlike distortions in the structure lead to antiferroelectric displacements for the O atoms along the b axis but an overall ferroelectric displacement along the a axis, in agreement with polarization measurements. While this simple model predicts the correct polarization for the C phase on the basis of the magnetic structure, the periodicity of the structural distortion suggests displacements of the Mn ions that cannot be accurately predicted in the absence of high-field crystallographic data. Finally, we note here that although in Fig. 1(b) we depict a collinear structure for simplicity, our neutron measurements show that indeed in the C-phase reflection types that arise from spiral components are visible but suppressed by a factor of 6 compared to the zero-field IC phase.

In this Communication we have demonstrated that the polarization flop in TbMnO_3 arises from a transition to a C phase with propagation vector $\kappa = (0, \frac{1}{4}, 0)$. The quadratic magnetoelastic coupling breaks down with field and the high-field phase exhibits linear magnetoelastic and magneto-electric behavior. We argue that field has the effect of releasing the apparent frustration in the orbital ordering in TbMnO_3 and leads to a C phase by an ordering of Mn–O–Mn bond angles.

Note added: Arima *et al.*¹⁷ recently reported some x-ray diffraction measurements for $H\parallel b$ similar to those described here.

The authors benefited from discussions with D. Khomskii, T. Kimura, and L.C. Chapon. We thank Klaus Habicht, Peter Smeibidl, Sebastian Gerischer, Klaus Kiefer, and Michael Meissner from BENSCH, C.J. Milne from HMI, and W.A. Caliebe from NSLS for assistance during the experimental work. Work at Brookhaven was supported by the U.S. Department of Energy, Division of Materials Science, under Contract No. DE-AC02-98CH10886.

¹T. Kimura *et al.*, Nature **426**, 55 (2003).

²T. Goto *et al.*, Phys. Rev. Lett. **92**, 257201 (2004).

³T. Kimura *et al.*, Phys. Rev. B **68**, 060403(R) (2003).

⁴N. Hur *et al.*, Nature **429**, 392 (2004).

⁵T. Lottermoser *et al.*, Nature **430**, 541 (2004).

⁶M. Kenzelmann *et al.*, Phys. Rev. Lett. **95**, 087206 (2005).

⁷S. Quezel *et al.*, Physica A **86-88**, 916 (1977).

⁸R. Kajimoto *et al.*, Phys. Rev. B **70**, 012401 (2004).

⁹M. L. Plumer and M. B. Walker, J. Phys. C **15**, 7181 (1982).

¹⁰M. B. Walker, Phys. Rev. B **22**, 1338 (1980).

¹¹T. Kimura *et al.*, Phys. Rev. B **71**, 224425 (2005).

¹²Y. Popov *et al.*, JETP Lett. **57**, 69 (1993).

¹³B. Ruetter *et al.*, Phys. Rev. B **69**, 064114 (2004).

¹⁴A. K. Zvezdin and A. P. Pyatakov, Phys. Usp. **47**, 416 (2004).

¹⁵J. Blasco *et al.*, Phys. Rev. B **62**, 5609 (2000).

¹⁶J. Goodenough, Phys. Rev. **100**, 564 (1955).

¹⁷T. Arima *et al.*, Phys. Rev. B **72**, 100102 (2005).